Nano-Structures & Nano-Objects 22 (2020) 100462

Contents lists available at ScienceDirect

Nano-Structures & Nano-Objects

journal homepage: www.elsevier.com/locate/nanoso

Magnetic nanoparticles in toner material

M. Getzlaff [a,*], M. Leifels [a], P. Weber [a], Ü. Kökcam-Demir [b], Ch. Janiak [b]

[a] Institute of Applied Physics, University of Düsseldorf, D-40225 Düsseldorf, Germany
[b] Institute of Inorganic and Structural Chemistry, University of Düsseldorf, D-40225 Düsseldorf, Germany

ARTICLE INFO

Article history:
Received 20 February 2020
Received in revised form 19 March 2020
Accepted 31 March 2020

Keywords:
Toner
Nanoparticles
Magnetic nanoparticles
Magnetite
Maghemite

ABSTRACT

Printers and copiers necessitate toner material which is device and therefore company dependent. These materials being part of everyday life and cheap exhibit different toner particles that are microscaled objects consisting of nanoparticles. The differences are related to the chemical composition, the shape and the size.

The first aim was to find toner material which contains magnetic substances. The subsequent goal of this investigation was a detailed examination of the material composition, the shape, the size, as well as a possible crystallinity of the micro- and nanoscaled particles from three different toner materials (distributed by Samsung, Hewlett–Packard, and Kyocera) all being commercially available. The background is aimed at the question whether these particles can be taken for magnetically related scientific investigations instead of carrying out complicated, long-lasting and expensive preparation procedures.

It could be demonstrated that cheap toner material can be used to obtain magnetic iron oxide nanoparticles of about 10 to 20 nm with a narrow size distribution using the investigated toner materials. With benzene, toluene, and n-hexane as organic solvent these nanoparticles are agglomerates of particles with a diameter being significantly below the micrometer size. Without dispersing one obtains large agglomerates of about 10 μm.

Using the toner material of Hewlett–Packard and Kyocera the metallic nanoparticles themselves exclusively consist of crystalline magnetite. Taking that of Samsung two configurations are present with about two thirds of magnetite and one third of maghemite.

1. Introduction

Printers and copiers necessitate toner material which is device and therefore company dependent. These materials being part of everyday life and cheap exhibit different toner particles that are microscaled objects consisting of nanoparticles [1]. The differences are related to the chemical composition, the shape and the size.

Therefore, one aspect is related to whether these (nano) particles are partially or totally magnetic [2,3]. A further one deals with the question whether they can be used for scientific investigations or applications like drug delivery [4], magnetic targeting [5], hyperthermia [6–8], thermal ablation [9], stem cell sorting and manipulation [10], gene therapy [11], MRI contrast enhancement [12], food preservation [13], bioprocess intensification [14,15], as antimicrobial agents [16], bioseparation [17], as ferrofluids [18], environmental remediation [19], lithium-ion batteries [20], as active electrode materials for supercapacitors [21], water purification [22], or as pigments [23] (further details can be found in corresponding reviews, e.g., [24–28]). This possibility to obtain magnetic nanoparticles with special properties would have significant advantages because the procedure is cheap and fast compared to other established preparation processes which use sophisticated set-ups like magnetron sources [29], arc cluster ion sources [30], or gas aggregation sources [31]. More experimental techniques as well as an overview can be found in [32]. These procedures require an ultra high vacuum (UHV) and a subsequent size or mass selection [33,34]. It should be noted that some wet chemical processes are also suitable [35–37].

In the case of iron oxide as magnetic particle material it is important to note that they are part of our ambience as well as often found in living systems like fishes (e.g., rainbow trouts) [38,39], birds (e.g., homing pigeons) [40,41], and magnetotactic bacteria [42–45]. Nanoparticles consisting of iron oxide are nowadays often used for applications in the field of nanomedicine. This is due to their large magnetic moments, properties concerning magnetic anisotropies, superparamagnetic behavior, extremely large surface-to-volume ratio, magneto thermal effects, as well as the above mentioned biocompatibility [46–49].

Iron oxide most commonly exists in the three configurations of hematite (α-Fe_2O_3), maghemite (γ-Fe_2O_3), and magnetite

* Corresponding author.
E-mail address: getzlaff@uni-duesseldorf.de (M. Getzlaff).

https://doi.org/10.1016/j.nanoso.2020.100462
2352-507X/

(Fe_3O_4). Particularly, magnetite nanoparticles are considered as promising magnetic nanoscaled objects for clinical and in-vivo applications because they exhibit a vanishing magnetism after switching-off an external magnetic field due to their superparamagnetic behavior.

As the initial step the chemical composition of the nanoparticles has to be clarified because it must be known which materials are offered in the different toner materials.

For nanoscaled objects every property significantly varies with the size [33,50], for example chemical [51], electronic [52], mechanical [33], magnetic [53,54], and optical properties [55–57], as well as the melting behavior [58].

As an important consequence it is not sufficient to get information on the size but it is additionally necessary to determine the size distribution. The corresponding key questions are therefore directed to the type of distribution (monomodal, bimodal, or multimodal), how broad are the distributions, in which way are properties influenced by different solvents, and which differences of toner material from different companies are present.

Thus, the aim is directed to the determination of the chemical composition especially relating to magnetic ingredients. A further one refers to the investigation of size, shape and crystallinity of the particles from different toner materials which are distributed by three companies using several respective methods.

Transmission electron microscopy (TEM) is used to determine the size being possible for small objects or thin samples. The shape of metallic objects can be imaged by scanning electron microscopy (SEM). For nanoparticles, the size can also be determined.

The determination of chemical elements in the toner material can be carried out by energy dispersive X-ray spectroscopy (EDX). A qualitative and also a (semi)quantitative analysis is possible using the X-rays emitted by the sample because their energy is characteristic of its element composition and the intensity of the respective amount. To generate the characteristic X-rays an X-ray tube or high-energy electrons of, e.g., transmission or scanning electron microscopes can be used.

X-ray diffraction (XRD) represents a powerful tool for the investigation of crystalline samples. Powder X-ray diffractometry enables to study polycrystalline materials. The use of monochromatic X-rays allows to evaluate specific Bravais lattices from both single element crystallites as well as a mixture of different compounds. This can be carried out if diffraction at different net planes takes place and taking the Bragg condition into account. The obtained lattice parameters are fingerprints enabling the determination of an element itself or the stoichiometry in case of alloys. Therefore, this information is gained in an independent way compared to EDX.

Dynamic light scattering (DLS) can be used to determine independently the size of micro- and nanosized particles in a solution. The diffusion coefficient of particles is obtained from the scattered light intensity. Larger particles exhibit a smaller diffusion coefficient, smaller ones a larger coefficient which can be understood due to the size dependence of the Brownian motion. Additionally, the size can be estimated making use of the Stokes–Einstein equation. It should be noted that particles in a solution carry a ligand shell that has an influence on the diffusion process. Therefore, the particles' size determined by DLS is larger than that by SEM and TEM.

2. Experimental details

Experimental techniques and technical equipment

The techniques being used (TEM, SEM, EDX, XRD, DLS) as well as the equipment was already described in [59].

Types of different toners

The toner CLT-K506L from Samsung is announced to be used for laser printers of the CLP and CLX series from Samsung. The toner HP 35A from Hewlett–Packard with code number CB435A is manufactured for the HP LaserJet series. The toner from Kyocera with the article number TK-12 can be used for laser printers of the FS series from Kyocera.

Sample preparation

The toner particles were directly removed from the fill of the printer toner of the respective cartridge. Subsequently, the material was put into plastic tubes. These were closed for further storage.

Neat samples

For PXRD and SEM/EDX investigations the respective toner material from the closed plastic tube was directly inserted into the measurement devices with no additional solvent.

PXRD. The neat sample was directly inserted into the diffractometer.

SEM. Few samples must be covered with gold (toner material of Kyocera) due to a too low conductivity. For the toner material from Samsung and Hewlett–Packard this additional step was not necessary because these samples exhibited a sufficient conductivity. The samples were put onto the holder of the SEM which is made of aluminum and brass. Therefore, all signals from these elements (Al, Cu, Zn, Au) in EDX measurements were not taken into data analysis due to their absence in the original toner material.

Dispersed samples

As preparative for DLS and TEM/EDX investigations a glass (Behr Labor-Technik GmbH; 20 ml) was filled with a small amount of the respective printer toner. Subsequently, one specific solvent (benzene, toluene or n-hexane) was added to the toner material until the sample became transparent due to suspension of the particles.

DLS. The dispersed sample was dripped into a glass cuvette which was subsequently covered with a cap to prevent evaporation of the solvent.

TEM. A drop of the dispersed sample was put onto a TEM copper grid (Plano GmbH; Formvar/Carbon film; 200 mesh).

Magnetic separation. A strong magnet was approached to the glass filled with the respective dispersed toner material.

3. Results

In this investigation three different toner materials were examined. Their properties will be presented in this chapter. Corresponding discussion and comparison related to the aspects given above are content of the subsequent chapter 4.

3.1. Toner samsung

No data sheet is available which declares the content of the toner material.

3.1.1. EDX

The chemical composition was determined using EDX. The obtained values are listed in Table 1. A high amount of Fe is present which hints to ferrite like magnetite.

Table 1
Chemical composition of the Samsung CLT-K506L toner material obtained by EDX.

Element	At. weight [%]	Uncertainty [%]
C	76.9	6.9
O	15.9	2.2
Fe	6.8	0.7
Other	0.4	

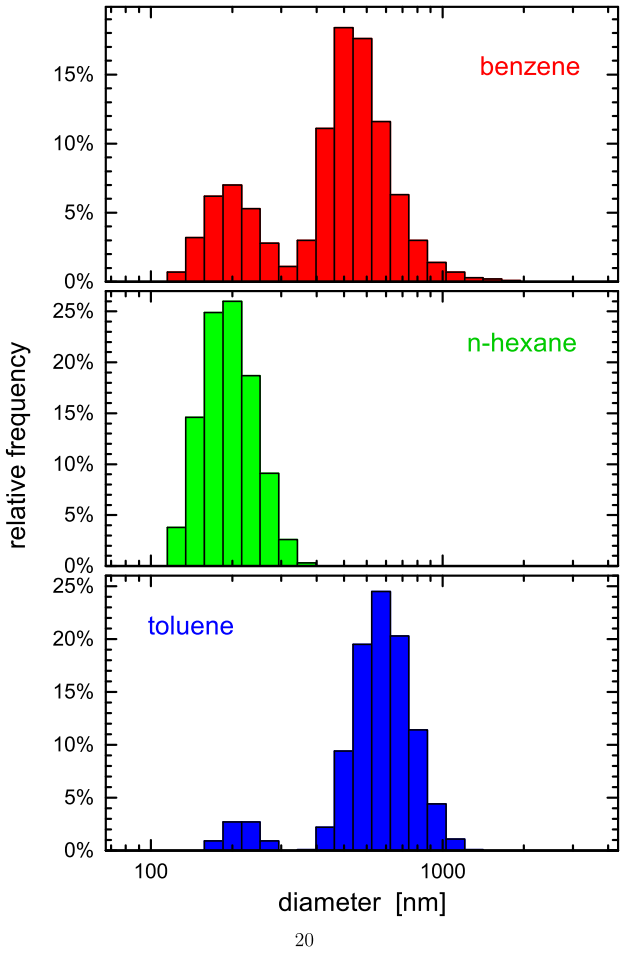

Fig. 1. Hydrodynamic diameters of the Samsung toner material dispersed in benzene (top), in n-hexane (middle) and in toluene (bottom) obtained by DLS.

3.1.2. DLS

The toner material was dispersed in benzene, in n-hexane as well as in toluene. DLS was used to determine the respective hydrodynamic diameters (s. Fig. 1) It is obvious that in all three solvents two size regimes are present only with different weighting. The two regimes are given by hydrodynamic diameters of about 200 nm and around 600 nm. In benzene the larger particles occur twice as much as the smaller ones. In n-hexane only the small particles can be observed thus representing a monomodal size distribution. In toluene only a small fraction of the smaller particles are present but most of them possess the large diameter.

The polydispersity index is about 0.46 using benzene as solvent which can be understood due to the two different sizes, i.e. the bimodal size distribution. With n-hexane as well as toluene as solvents it amounts to about 0.28 being significantly lower due to the monomodal size distribution. This value is between 0.1 and 0.4. Consequently, the distribution lies in an intermediate range and is therefore neither extremely polydisperse, or broad, nor in any sense narrow.

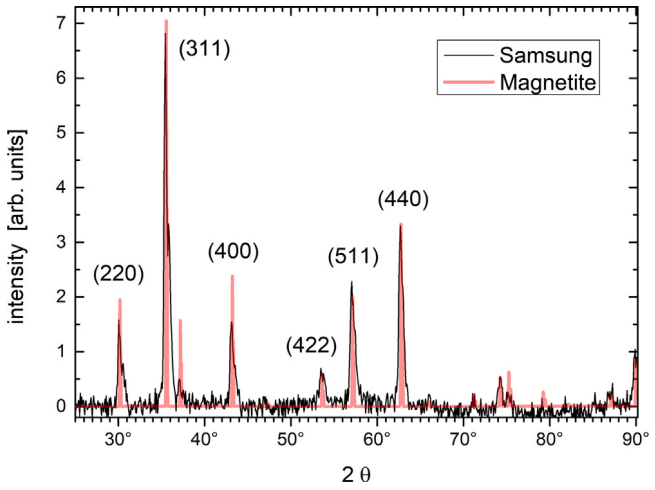

Fig. 2. Powder X-ray diffraction pattern of the Samsung toner material after background subtraction (black curve). The reference diffractogram of magnetite is additionally shown (red bars). The corresponding diffraction planes are additionally given. (For interpretation of the references to colour in this figure legend, the reader is referred to the web version of this article.)

3.1.3. PXRD

Powder X-ray diffraction measurements were carried out for the determination of the crystallinity of the toner material (s. Fig. 2). The black curve shows the diffraction intensity of the toner material after background subtraction. The red curve represents the pattern of magnetite, the values were obtained from the RRUFF database (R061111) with the corresponding diffraction planes. All peaks can be reproduced with the reference spectrum and no additional feature occurs. At about 21° no peak can be observed which proves that crystalline silica does not exist as found for toner materials from other companies [59]. Therefore, it can be concluded that the crystalline material in the toner seems to consist of magnetite. No broad structure is present pointing to the absence of amorphous material. Additionally, the peaks are not symmetric but exhibit a shoulder on the high-angle side.

The most prominent peak of the diffraction pattern from (311) is used to estimate the size of the crystalline particles using the Scherrer equation

$$d = \frac{K \cdot \lambda}{w \cdot \cos\theta} \tag{1}$$

with K the Scherrer constant, λ the wavelength of the X-rays, w the width (e.g., the full width at half maximum FWHM), and d the diameter of the nanoparticle. It should be noted that in this equation w is given in rad. A proportionality factor of 57.3 must be taken into account for values in degree. The double-peak structure is directly to be seen (s. Fig. 3). The black line represents the measurement of the toner material, the colored curves a fit with two Gaussian functions. The red and green curve are the two single Gaussian functions and the blue one the sum. The data can be reproduced very well. The fit results in an angle of $(35.4 \pm 0.1)°$ and a width (FWHM) of $(0.41 \pm 0.04)°$ for the first and an angle of $(35.9 \pm 0.1)°$ and a width of $(0.41 \pm 0.04)°$ for the second peak. As Scherrer constant being typical for spherical particles with cubic symmetry a value of K of 0.94 was chosen. The obtained diameters amount to (21 ± 2) nm using the first and to (21 ± 2) nm using the second peak. The intensity ratio is about 0.44.

The same procedure was carried out for the pattern of the (440) plane at about 63° (s. Fig. 4). This fit results in an angle of $(62.6 \pm 0.1)°$ and a width (FWHM) of $(0.35 \pm 0.04)°$ for the first and an angle of $(63.0 \pm 0.1)°$ and a width of $(0.35 \pm 0.04)°$ for the

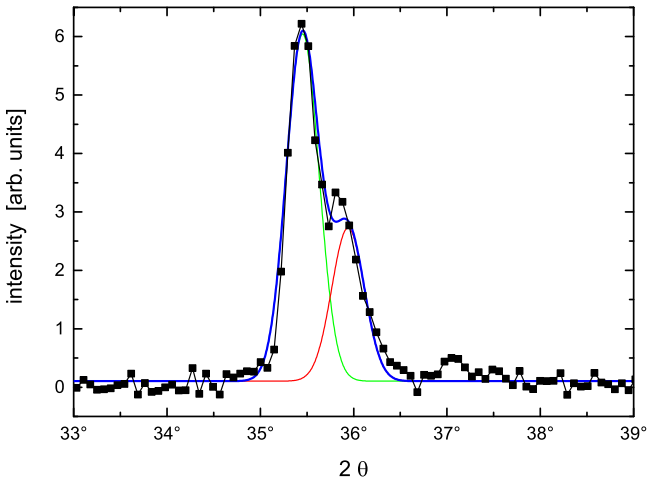

Fig. 3. Powder diffraction pattern of Samsung toner material in the angle range between 33° and 39° (black line). The most prominent peak was fitted with two Gaussian functions (blue line). (For interpretation of the references to colour in this figure legend, the reader is referred to the web version of this article.)

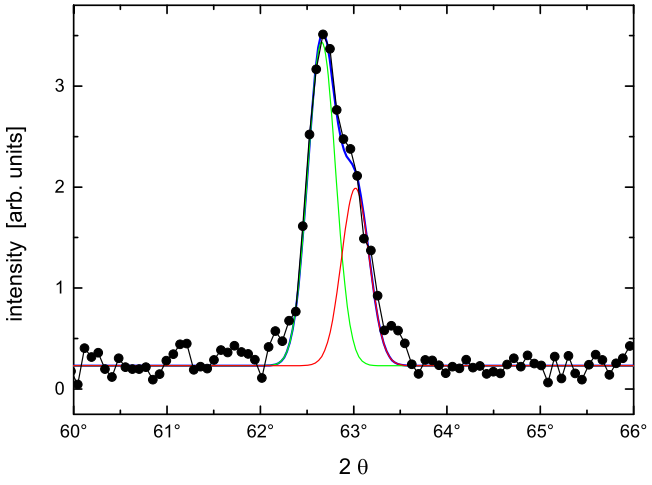

Fig. 4. Powder diffraction pattern of Samsung toner material in the angle range between 60° and 66° (black line). The most prominent peak was fitted with two Gaussian functions (blue line). (For interpretation of the references to colour in this figure legend, the reader is referred to the web version of this article.)

second peak. The obtained diameters amount to (28±3) nm using the first and to (28 ± 3) nm using the second peak. The relative intensity of the second peak is about 0.54 of that of the first peak.

3.1.4. TEM

The TEM image of the toner material being dispersed in benzene is given in Fig. 5. Large agglomerates can be seen exhibiting a size of about 200 nm. Due to the strong absorption they do not consist of light elements like C but more likely of heavier ones (like, e.g., Fe).

3.1.5. SEM

The investigation of the toner material by SEM was carried out without (previous) dispersion (s. Fig. 6). The left part shows irregularly shaped particles with sizes between about 5 μm and 10 μm. Using a higher magnification (right part) it can be seen that they are made up of smaller particles.

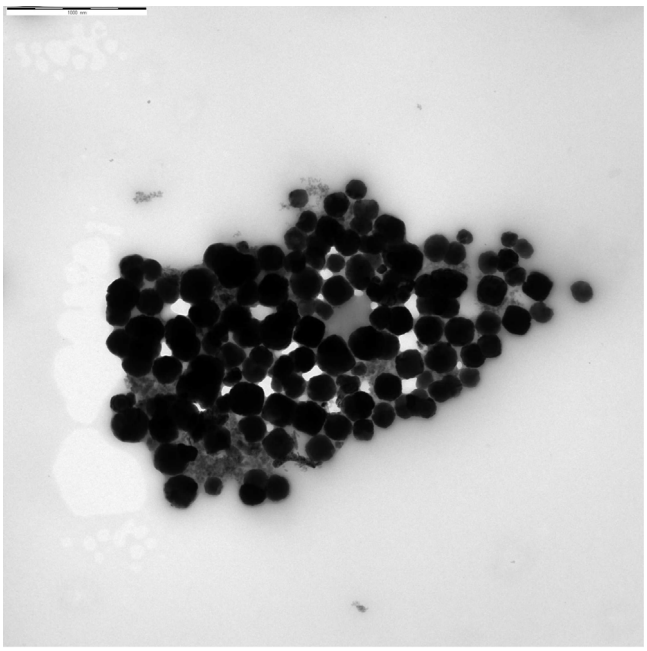

Fig. 5. TEM image of the Samsung toner material dispersed in benzene (scale bar: 1000 nm).

3.1.6. Conclusion

The chemical composition taken from EDX/SEM measurements proves C, O and Fe; the comparison with a data sheet cannot be done because it was not available.

This result is in agreement with PXRD investigations which proved the existence of crystalline material being exclusively iron oxide.

The double-peak structures can be understood if it is assumed that not exclusively magnetite is present but also γ-Fe_2O_3 (maghemite). Using the American Mineralogist Crystal Structure Database (amcsd) one finds that for the used excitation energy the two most intense diffraction peaks are at 35.47° with a relative intensity of 100 and at 62.60° with a relative value of 42.1 for magnetite (amcsd 0020587). For maghemite (amcsd 0020518) these structures are at 35.68° with a relative intensity of 100 and at 63.01° with a relative value of 40.4.

Therefore, the peak at each low-angle side is due to magnetite particles. The measured angles of 35.4° and 62.6° are in good agreement to the database values of 35.47° and 62.60°. Additionally, the measured intensity ratio amounts to 0.46 also in good agreement to the database being 0.42. The average value of the diameter results in (25 ± 3) nm for the magnetite particles.

The peak at each high-angle side is related to maghemite particles. Measured angles in this investigation are 35.9° and 63.0°. They are in good agreement to the database values of 35.68° and 63.01°. Additionally, the measured intensity ratio amounts to 0.55 being in agreement to the database value being 0.40. The average value of the diameter results in (25 ± 3) nm for the maghemite particles.

The comparison of the intensities between both kinds of particles results in a relative ratio for the maghemite particles of about 0.44 for the first and of about 0.54 of the second peak. That means that the observed patterns are due to the two coexisting configurations magnetite and maghemite with the respective ratio of 2 : 1.

The SEM measurements show that the toner powder is built up of large agglomerates with a size of about 5-10 μm which exhibit smaller particles. In a dispersion these large particles are

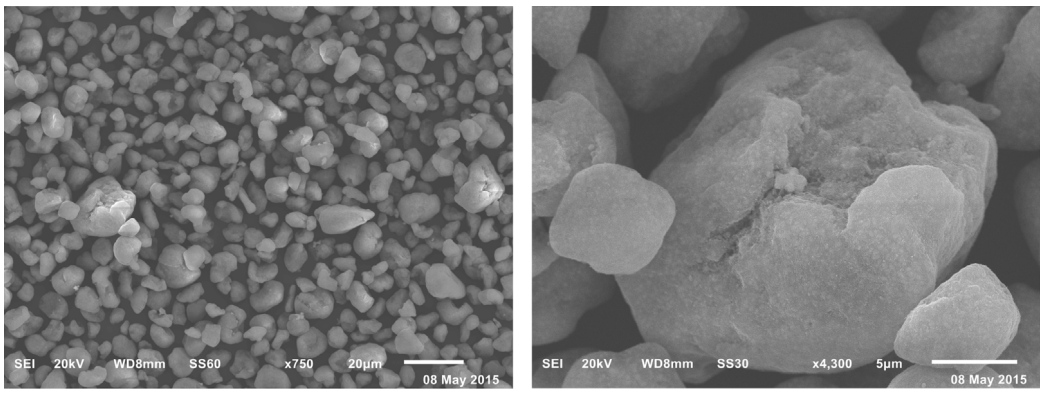

Fig. 6. SEM images of the Samsung toner material without a previous dispersion. Left: Scale bar: 20 µm. Right: Scale bar: 5 µm.

Table 2
Chemical composition of the Hewlett–Packard 35A toner material obtained by EDX.

Element	At. weight [%]	Uncertainty [%]
C	75.5	7.8
O	19.1	3.0
Fe	5.2	0.6
other	0.2	0.1

not observable. It points to that they consist of particles which are dispersed in the respective solvent which was obvious using DLS. This measurement proved different hydrodynamic diameters after dispersion in benzene and toluene with 200 nm and 600 nm, i.e., a bimodal distribution, and in n-hexane with about 200 nm. Additionally, TEM investigations confirmed particles with diameters of about 200 nm. These are built up of small nanoparticles of crystalline material which was proven by PXRD. The Scherrer equation using the width of the PXRD diffraction peaks results in a diameter of about 25 nm for magnetite as well as for maghemite nanoparticles.

3.2. Toner Hewlett–Packard

From the data sheet one could see that the content consists of ferrite, styrene acrylate copolymer and wax. There was no declaration of the respective relative amount.

3.2.1. EDX

The chemical composition was determined by EDX . The obtained values are listed in Table 2. All detected elements were stated as components in the data sheet.

3.2.2. DLS

Dynamic light scattering measurements were carried out to determine the hydrodynamic diameter of the toner particles (s. Fig. 7). It is obvious that a multimodal size distribution is present. Small particles with a hydrodynamic diameter of about 20 nm and others with about 80 nm can be found. Also larger particles occur with diameters of around 300 nm and most likely agglomerates with a size of about several µm can be observed.

3.2.3. PXRD

Powder X-ray diffraction measurements were carried out for the determination of the crystallinity of the toner material (s. Fig. 8). The black curve shows the diffraction intensity of the toner material after background subtraction. The red curve represents the pattern of magnetite, the values were obtained from the RRUFF database (R061111) with the corresponding diffraction

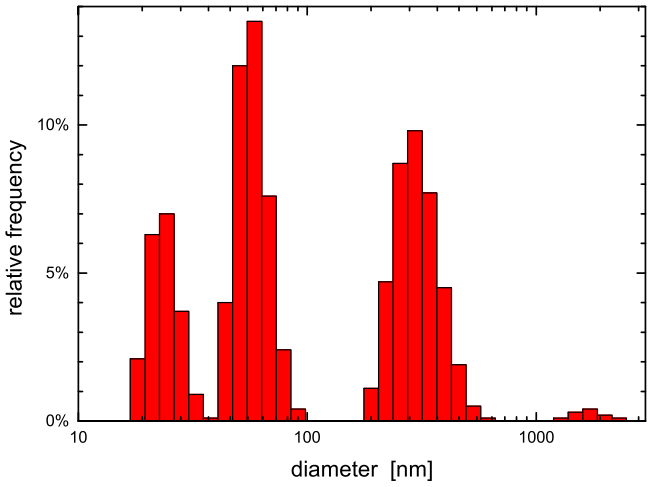

Fig. 7. Hydrodynamic diameter of Hewlett–Packard toner material being dispersed in benzene and obtained by DLS.

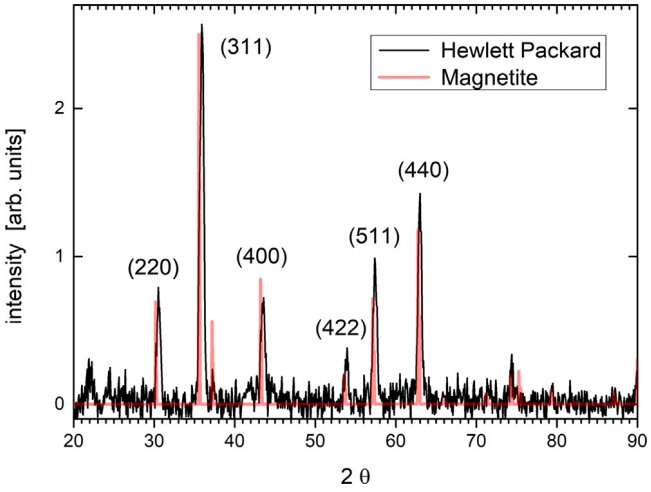

Fig. 8. Powder X-ray diffraction pattern of the Hewlett–Packard toner material after background subtraction (black curve). The reference diffractogram of magnetite is additionally given (red bars). The corresponding diffraction planes are given, too. (For interpretation of the references to colour in this figure legend, the reader is referred to the web version of this article.)

planes. All peaks can be reproduced with the reference spectrum (a small shift of about 0.3° may be due to an experimental misalignment) and no additional sharp feature occurs. Therefore,

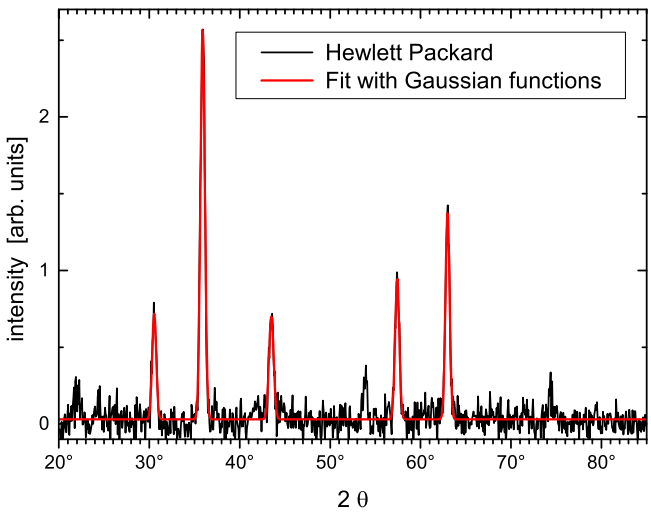

Fig. 9. Powder diffraction pattern of Hewlett–Packard toner material in the angle range between 20° and 85° (black line). The most prominent peaks were fitted with Gaussian functions (red line). (For interpretation of the references to colour in this figure legend, the reader is referred to the web version of this article.)

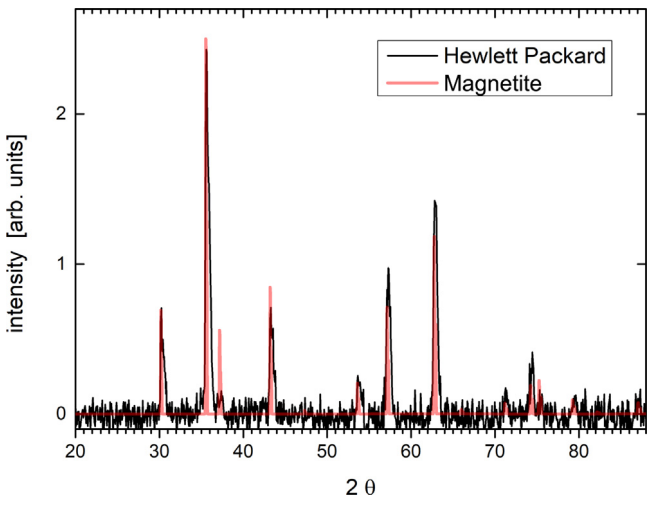

Fig. 10. Powder X-ray diffraction pattern of the Hewlett–Packard toner material *after magnetic separation* and background subtraction (black curve). The reference diffractogram of magnetite is additionally given (red bars). (For interpretation of the references to colour in this figure legend, the reader is referred to the web version of this article.)

it can be concluded that the crystalline material in the toner exclusively consists of magnetite. No broad structure is present pointing to the absence of amorphous material.

The five most prominent peaks of the diffraction pattern related to the (220), (311), (400), (511), and (440) planes are used to estimate the size of the crystalline particles using the Scherrer equation (s. Eq. (1)). The black line represents the measurement of the toner material, the red curve a fit with five Gaussian functions (s. Fig. 9) which can reproduce the data very well. The fit results in an angle of $(30.5 \pm 0.1)^\circ$ and a width (FWHM) of $(0.53 \pm 0.04)^\circ$ for the first peak of the (220) plane, an angle of $(35.9 \pm 0.1)^\circ$ and a width of $(0.58 \pm 0.01)^\circ$ for the second peak of the (311) plane, an angle of $(43.5 \pm 0.2)^\circ$ and a width of $(0.61 \pm 0.04)^\circ$ for the third peak of the (400) plane, an angle of $(57.4 \pm 0.1)^\circ$ and a width of $(0.55 \pm 0.03)^\circ$ for the fourth peak of the (511) plane and an angle of $(63.0 \pm 0.1)^\circ$ and a width of $(0.53 \pm 0.02)^\circ$ for the fifth peak of the (440) plane. As Scherrer constant a value of K of 0.94 was chosen. The obtained diameters amount to (16 ± 1) nm for the first, to (15 ± 1) nm for the second, to (15 ± 1) nm for the third, to (17 ± 1) nm for the fourth and to (18 ± 1) nm for the fifth peak. This determination leads to an average value of (16 ± 1) nm.

In order to distinguish the magnetic from possible nonmagnetic particles a magnetic separation was carried out exemplarily for this toner material by means of a strong magnet for the dispersed sample. Subsequently, a drying procedure was carried out and the X-ray diffraction measurements were done (s. Fig. 10). The comparison of the results before (s. Fig. 8) and after separation shows that no differences are present.

3.2.4. TEM

TEM images of the toner material which was dispersed in benzene are presented in Fig. 11. The left image shows that particles are present with a diameter of about 200 nm. They consist of smaller ones (s. right part) with a size of about 20 nm. EDX measurements (in a HR-TEM) on individual nanoparticles prove a composition of Fe and O.

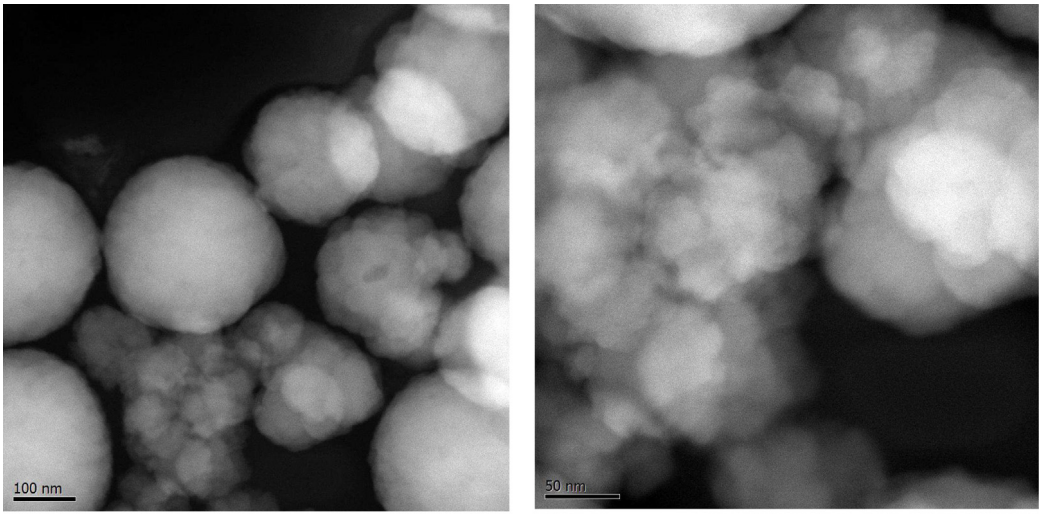

Fig. 11. TEM image of Hewlett–Packard toner material dispersed in benzene. Left: Scale bar: 100 nm. Right: Scale bar: 50 nm.

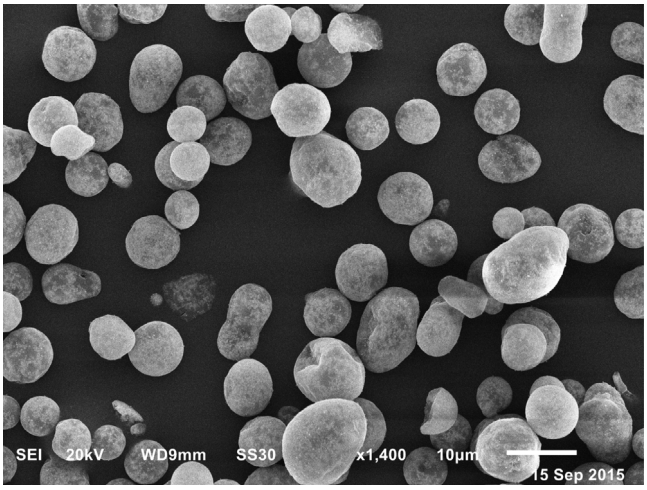

Fig. 12. SEM images of the Hewlett–Packard toner material without a previous dispersion (scale bar: 10 µm).

Table 3
Chemical composition of the Kyocera toner material obtained by EDX. The most prominent elements are C, O and Fe. The relative amount of others like Si and Al is below 0.2% each.

Element	At. weight [%]	Uncertainty [%]
C	91.0	9.6
O	6.9	1.4
Fe	1.2	0.2
other	0.9	

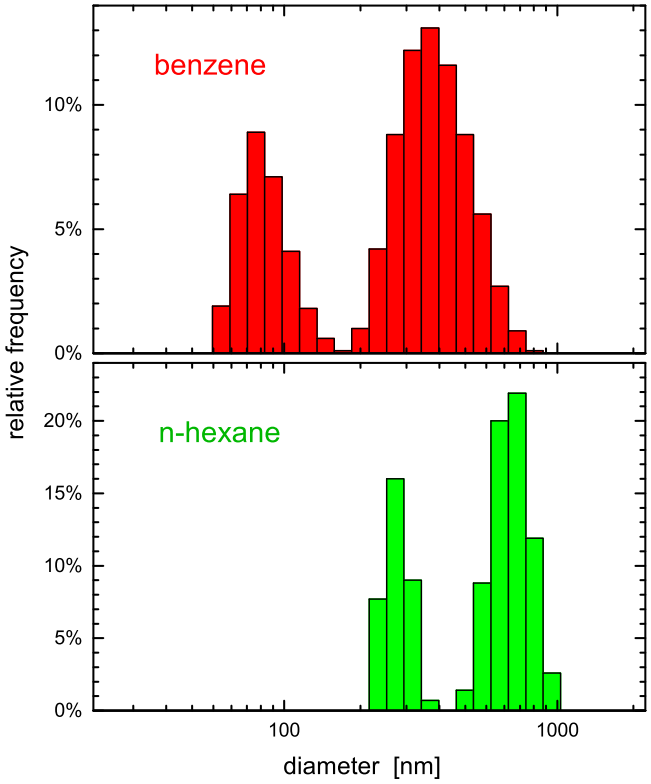

Fig. 13. Hydrodynamic diameter of Kyocera toner material obtained by DLS. Top: Dispersed in benzene. Bottom: Dispersed in n-hexane.

3.2.5. SEM

SEM was used to determine shape and size of the neat particles being in the Hewlett–Packard toner material (s. Fig. 12). The left part indicates particles exhibiting a size around 5 µm to 10 µm with a nearly spherical shape.

3.2.6. Conclusion

The chemical composition was determined with different experimental techniques all resulting in the same elements. EDX with SEM and also with HR-TEM as well as PXRD proves the exclusive existence of C, Fe, and O. This is in agreement with the data sheet.

Large particles of about several µm in size are present in the powder without a previous dispersion. After dispersion the toner particles in benzene one gets submicron-sized agglomerates consisting of nanoparticles of about 20 nm. According to DLS the agglomerates dispersed in benzene exhibit a trimodal size distribution of in average 20 nm, 80 nm and 300 nm. This points to small aggregates which consist of several nanoparticles with 20 nm in diameter. It is corroborated from PXRD measurements which prove crystalline nanoparticles with a size of about 16 nm being determined from the width of the diffraction peaks using the Scherrer equation.

3.3. Toner kyocera

The content can be found in the data sheet to be acrylic copolymer, polypropylene wax, carbon black, magnetite, alumina and silica. The respective relative amount was not given.

3.3.1. EDX

The chemical composition was determined by EDX. The obtained values are listed in Table 3. All detected elements are part of the components stated in the data sheet.

3.3.2. DLS

For the determination of the hydrodynamic diameter of the toner particles dynamic light scattering measurements were carried out (s. Fig. 13). The upper histogram shows the sizes of the particles dispersed in benzene. Two different size regimes can be found with about 80 nm and around 400 nm. After dispersion of the material in n-hexane (bottom diagram) one also obtains a bimodal size distribution with about 250 nm and around 700 nm. With benzene as solvent the polydispersity index is about 0.39 whereas with n-hexane as solvent it amounts to about 0.48. Both values can be understood due to the two different sizes, i.e. the bimodal size distribution.

3.3.3. PXRD

Powder X-ray diffraction measurements were carried out for the determination of the crystallinity of the toner material (s. Fig. 14) The black curve shows the diffraction intensity of the toner material after background subtraction. The red curve represents the pattern of magnetite, the values were obtained from the RRUFF database (R061111) with the corresponding diffraction planes. All peaks can be reproduced with the reference spectrum and no additional feature occurs. At about 21° no peak can be observed which proves that crystalline silica does not exist in the toner. Therefore, it can be concluded that the crystalline material in the toner consists of magnetite only. No broad structure is present pointing to the absence of amorphous material.

The five most prominent peaks of the diffraction pattern are used to estimate the size of the crystalline particles using the Scherrer equation (s. Eq. (1)). The black line represents the measurement of the toner material, the red curve a fit with five Gaussian functions (s. Fig. 15) which can reproduce the data very well. The fit results in an angle of $(30.2 \pm 0.1)°$ and a width (FWHM) of $(1.26 \pm 0.02)°$ for the first peak of the (220) plane,

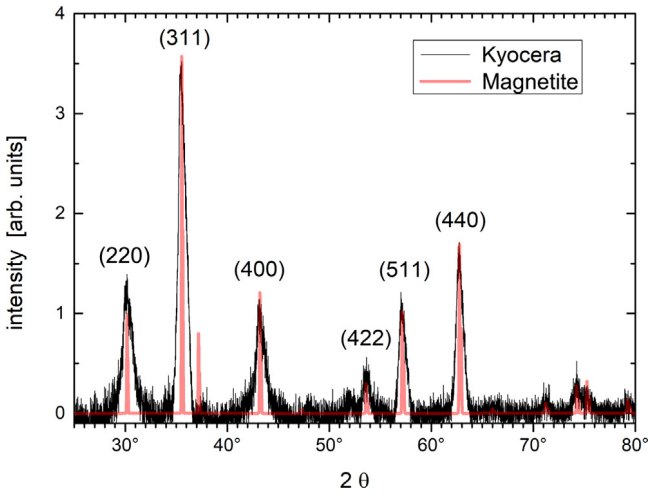

Fig. 14. Powder X-ray diffraction pattern of the Kyocera toner material after background subtraction (black curve). The reference diffractogram of magnetite is additionally given (red bars). The corresponding diffraction planes are shown, too. (For interpretation of the references to colour in this figure legend, the reader is referred to the web version of this article.)

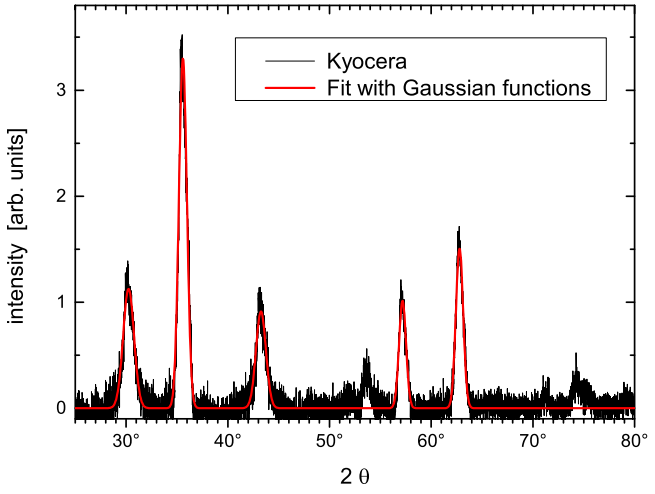

Fig. 15. Powder diffraction pattern of Kyocera toner material in the angle range between 25° and 80° (black line). The most prominent peaks were fitted with Gaussian functions (red line). (For interpretation of the references to color in this figure legend, the reader is referred to the web version of this article.)

an angle of $(35.6 \pm 0.1)°$ and a width of $(0.92 \pm 0.01)°$ for the second peak of the (311) plane, an angle of $(43.3 \pm 0.1)°$ and a width of $(1.15 \pm 0.02)°$ for the third peak of the (400) plane, an angle of $(57.2 \pm 0.1)°$ and a width of $(0.81 \pm 0.02)°$ for the fourth peak of the (511) plane and an angle of $(62.8 \pm 0.1)°$ and a width of $(0.84 \pm 0.01)°$ for the fifth peak of the (440) plane. As Scherrer constant a value of K of 0.94 was chosen. The obtained diameters amount to (6 ± 1) nm for the first, to (10 ± 1) nm for the second, to (8 ± 1) nm for the third, to (12 ± 1) nm for the fourth and to (12 ± 1) nm for the fifth peak. This determination leads to an average value of (10 ± 1) nm.

3.3.4. TEM

A TEM image of Kyocera toner material after dispersion in benzene is shown in Fig. 16. Small particles are present with a size of about 100 nm which are agglomerated to larger ones with a dimension of around 200 nm.

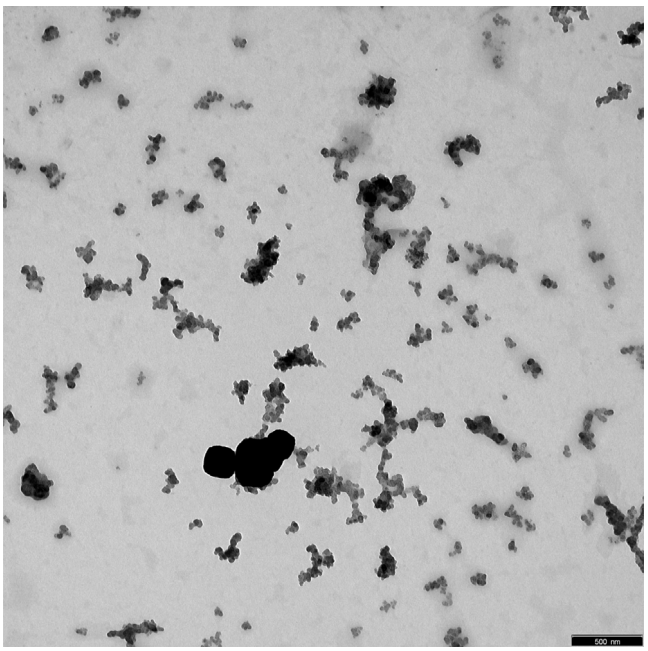

Fig. 16. TEM image of Kyocera toner material dispersed in benzene (scale bar: 500 nm).

3.3.5. SEM

SEM was used to determine the shape and size of the neat particles being in the Kyocera toner material (s. Fig. 17). The image shows irregularly shaped particles with sizes between about several and 10 μm.

3.3.6. Conclusion

The chemical composition was determined by EDX/SEM to be C, O and Fe; the comparison with a data sheet shows a good agreement. This result corroborates the PXRD investigations which demonstrate that crystalline material is present which is exclusively made up of iron oxide in the configuration of magnetite.

The toner powder consists of large particles with a size of about 10 μm which seem to exhibit smaller particles as proven by SEM. In a solution these large particles are not observable. Therefore, the large agglomerates can be dispersed in the respective solvent. This was proven using DLS which led to significantly smaller, but different hydrodynamic diameters after dispersion in benzene with 80 nm and 400 nm and in n-hexane with about 250 nm and 700 nm. Thus, in both situations a bimodal distribution is present. An confirmation TEM investigations showed particles after dispersion in benzene with diameters of 100 nm and about 200 nm. These are built up of small nanoparticles of crystalline magnetite which was proven by PXRD. The Scherrer equation results in a diameter of about 10 nm.

4. Discussion

EDX confirmed that C, O, and Fe is present in the material of all three toners. More metallic components could not be found. PXRD allowed to determine the respective configurations. All crystalline nanoparticles exclusively consist of iron oxide.

In the toner material from Hewlett–Packard and Kyocera only magnetite is present, in that from Samsung the two configurations magnetite and maghemite can be found. Every dry toner dust contains particles with a size of approximately 10 μm being agglomerates of considerably smaller particles.

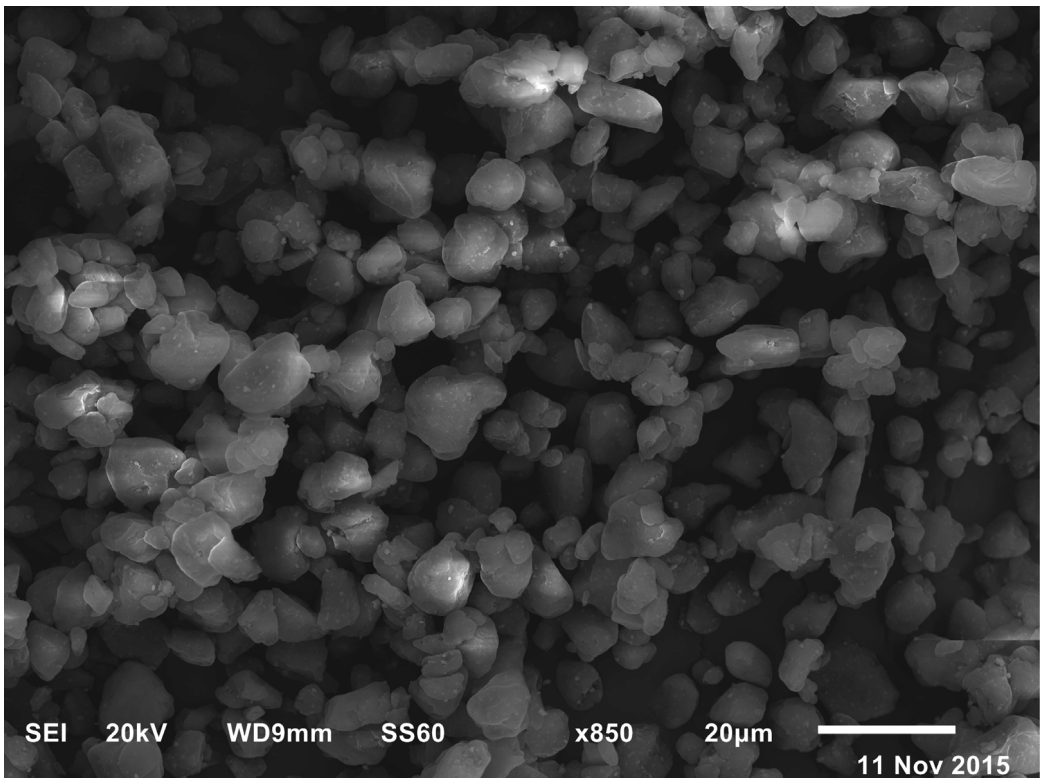

Fig. 17. SEM images of the Kyocera toner material without a previous dispersion (scale bar: 20 μm).

It was not possible to disperse the toner dust in water. The explanation is given due to the insolubility of iron oxide in water [60]. Therefore, only solvents were used which are rather nonpolar. In order to determine the dependence on the degree of polarity n-hexane, toluene, and benzene (the solubility in water is about 10 mg/ℓ for n-hexane, 520 mg/ℓ for toluene, and 1770 mg/ℓ for benzene) [60] were taken. It was possible to disperse every toner material in all three liquids. Another explanation could be that this nanomaterial is yet more or less dispersible in water. The lack of dispersability may come from the association of the magnetic nanoparticles to the polymeric components of toner.

Being dispersed in benzene the particles of all three toner materials are made up of smaller agglomerates with a preferred size of around 200 nm which consist of crystalline nanoparticles of about 20 nm. The properties of the different solubilities allows to understand the different weighting in the bimodal distribution of the particles of the Samsung toner material. In n-hexane only particles with a size of 200 nm exist due to the best dispersion parameters. In benzene and toluene, the dispersion is not so good which is reflected by the bimodal distribution with a second fraction at a size of about 600 nm.

Therefore, it could be shown that cheap toner material can be used to obtain iron oxide nanoparticles of about 10 to 20 nm with a narrow size distribution using the investigated toner material from Samsung, Hewlett–Packard, and Kyocera. With n-hexane, toluene, and benzene as solvent they are agglomerated to particles significantly below the micrometer size. Without dispersion one obtains large agglomerates of about 10 μm. The trend of the material to self-agglomerate is an indication of how active is the surface of the nanoparticles which may need further chemical modification (addition of a surfactant) in order to stabilize them.

Using the toner material of Hewlett–Packard and Kyocera the nanoparticles themselves exclusively consist of crystalline magnetite. Taking that of Samsung two configurations are present with about two thirds of magnetite and one third of maghemite.

5. Summary

Printers and copiers necessitate toner material which is device and therefore company dependent. These materials being part of everyday life and cheap exhibit different toner particles that are microscaled objects consisting of nanoparticles. The differences are related to the chemical composition, the shape and the size.

The first aim was to find toner material which contains magnetic substances. The subsequent goal of this investigation was a detailed examination of the material composition, the shape, the size, as well as a possible crystallinity of the micro- and nanoscaled particles from three different toner materials (distributed by Samsung, Hewlett–Packard, and Kyocera) all being commercially available. The background is aimed at the question whether these particles can be taken for magnetically related scientific investigations instead of carrying out complicated, long-lasting and expensive preparation procedures.

It could be demonstrated that cheap toner material can be used to obtain magnetic iron oxide nanoparticles of about 10 to 20 nm with a narrow size distribution using the investigated toner materials. With n-hexane, toluene, and benzene as solvent they are agglomerated to particles significantly below the micrometer size. Without dispersing one obtains large agglomerates of about 10 μm.

Using the toner material of Hewlett–Packard and Kyocera the metallic nanoparticles themselves exclusively consist of crystalline magnetite. Taking that of Samsung two configurations are present with about two thirds of magnetite and one third of maghemite.

Declaration of competing interest

The authors declare that they have no known competing financial interests or personal relationships that could have appeared to influence the work reported in this paper.

Acknowledgments

We would like to thank Karsten Klauke (University of Düsseldorf) for some XRD investigations as well as Dennis Dietrich (University of Düsseldorf) for SEM/EDX measurements, further Martina Pohl (University of Rostock) for taking HR-TEM images and Marion Nissen (Center of Advanced Imaging CAi at the University of Düsseldorf) for TEM measurements.

References

[1] A. Koivisto, T. Hussein, R. Niemelä, T. Tuomi, K. Hämeri, Atmos. Environ. 44 (2010) 2140.
[2] U. Meisen, H. Kathrein, J. Imaging Technol. 44 (2000) 508.
[3] J. Hornak, Magn. Res. Imaging 25 (2007) 1459.
[4] L. Yang, Z. Cao, H. Sajja, H. Mao, L. Wang, H. Geng, H. Xu, T. Jiang, W. Wood, S. Nie, Y. Wang, J. Biomed. Nanotechnol. 4 (2008) 439.
[5] N. Ebrahimi, S. Rasoul-Amini, A. Ebrahiminezhad, Y. Ghasemi, A. Gholami, H. Seradj, Acta Metall. Sin. 29 (2016) 326.
[6] R. Hergt, R. Hiergeist, I. Hilger, W. Kaiser, Y. Lapatnikov, S. Margel, U. Richter, J. Magn. Magn. Mater. 270 (2004) 345.
[7] S. Laurent, S. Dutz, U. Häfeli, M. Mahmoudi, Adv. Colloid Interface Sci. 166 (2011) 8.
[8] E. Muzquiz-Ramos, V. Guerrero-Chavez, B. Macias-Martinez, C. Lopez-Badillo, L. Garcia-Cerda, Ceram. Int. 41 (2015) 397.
[9] I. Hilger, R. Hiergeist, R. Hergt, K. Winnefeld, H. Schubert, W. Kaiser, Invest. Radiol. 37 (2002) 580.
[10] Y. Pan, X. Du, F. Zhao, B. Xu, Chem. Soc. Rev. 41 (2012) 2912.
[11] J. Dobson, Gene Therapy 13 (2006) 283.
[12] N. Lee, T. Hyeon, Chem. Soc. Rev. 41 (2012) 2575.
[13] M. Busolo, J. Lagaron, Innov. Food Sci. Emerg. Technol. 16 (2012) 211.
[14] A. Ebrahiminezhad, V. Varma, S. Yang, Y. Ghasemi, A. Berenjian, Nanomaterials 6 (2016) 1.
[15] A. Ebrahiminezhad, V. Varma, S. Yang, A. Berenjian, Appl. Microbiol. Biotechnol. 100 (2016) 173.
[16] A. Ebrahiminezhad, S. Davaran, S. Rasoul-Amini, J. Barar, M. Moghadam, Y. Ghasemi, Curr. Nanosci. 8 (2015) 868.
[17] H. Yang, S. Zhang, X. Chen, Z. Zhuang, J. Xu, X. Wang, Anal. Chem. 76 (2004) 1316.
[18] M. Bautista, O. Bomati-Miguel, X. Zhao, M. Morales, T. Gonzales-Carreno, R.P. d. Alejo, J. Ruiz-Cabello, S. Veintemillas-Verdaguer, Nanotechnology 15 (2004) S154.
[19] T. Poursaberi, M. Hassanisadi, F. Nourmohammadian, Prog. Color Colorants Coat. 5 (2012) 35.
[20] G. Grinbom, D. Duveau, G. Gershinsky, L. Monconduit, D. Zitoun, Chem. Mater. 27 (2015) 2703.
[21] J. Theerthagiri, G. Durai, T. Tatarchuk, M. Sumathi, P. Kuppusami, J. Qin, M. Choi, Ionics (2019) http://dx.doi.org/10.1007/s11581--019--03330--9.
[22] T. Tatarchuk, I. Mironyuk, V. Kotsyubynsky, A. Shyichuk, M. Myslin, V. Boychuk, J. Mol. Liq. 297 (2020) 111757.
[23] L. Dengxin, G. Guolong, M. Fanling, J. Chong, J. Hazard. Mater. 155 (2008) 369.
[24] E. Abenojar, S. Wickramasinghe, J. Bas-Concepcion, Prog. Nat. Sci. Mater. Int. 26 (2016) 440.
[25] Z. Hedayatnasab, F. Abnisa, W. Daud, Mater. Des. 123 (2017) 174.
[26] H. Shokrollahi, J. Magn. Magn. Mater. 426 (2017) 74.
[27] L. Mohammed, H. Gomaa, D. Ragab, J. Zhu, Particuology 30 (2017) 1.
[28] A. Ebrahiminezhad, A. Zare-Hoseinabadi, A. Sarmah, S. Taghizadeh, Y. Ghasemi, A. Berenjian, Mol. Biotechnol. 60 (2018) 154.
[29] H. Haberland, M. Karrais, M. Mall, Y. Thurner, J. Vac. Sci. Technol. A 10 (1992) 3266.
[30] R. Methling, V. Senz, E. Klinkenberg, T. Diederich, J. Tiggesbäumker, G. Holzhüter, J. Bansmann, K. Meiwes-Broer, Eur. Phys. J. D 16 (2001) 173.
[31] S. Baker, S. Thornton, K. Edmonds, M. Maher, C. Norris, C. Binns, Rev. Sci. Instrum. 71 (2000) 3178.
[32] C. Binns, Surf. Sci. Rep. 44 (2001) 1.
[33] W. de Heer, Rev. Modern Phys. 65 (1993) 611.
[34] J. Bansmann, S. Baker, C. Binns, J. Blackman, J. Bucher, J. Dorantes-Davila, V. Dupuis, L. Favre, D. Kechrakos, A. Kleibert, K.-H. Meiwes-Broer, G. Pastor, A. Perez, O. Toulemonde, K. Trohidou, J. Tuaillon, Y. Xie, Surf. Sci. Rep. 56 (2005) 189.
[35] S. Sun, C. Murray, D. Weller, L. Folks, A. Moser, Science 287 (2001) 1989.
[36] H. Itoh, T. Sugimoto, J. Colloid Interface Sci. 265 (2003) 283.
[37] J. Vidal-Vidal, J. Rivas, M. Lopez-Quintela, Colloids Surf. A 288 (2006) 44.
[38] M. Walker, C. Diebel, C. Haugh, P. Pankhurst, J. Montgomery, C. Green, Nature 390 (1997) 371.
[39] C. Diebel, R. Proksch, C. Green, P. Neilson, M. Walker, Nature 406 (2000) 299.
[40] G. Fleissner, G. Fleissner, B. Stahl, G. Falkenberg, J. Ornithol. 148 (2007) S643.
[41] G. Falkenberg, G. Fleissner, K. Schuchardt, M. Kuehbacher, P. Thalau, H. Mouritsen, D. Heyers, G. Wellenreuther, G. Fleissner, PLoS One 5 (2010) e9231.
[42] D. Bazylinski, R. Frankel, Nat. Rev. Microbiol. 2 (2004) 217.
[43] D. Faivre, D. Schüler, Chem. Rev. 108 (2008) 4875.
[44] L. Yan, S. Zhang, P. Chen, H. Liu, H. Yin, H. Li, Microbiol. Res. 167 (2012) 507.
[45] S. Dasdag, H. Bektas, J. Phys. Chem. Biophys. 4 (2014) 1000141.
[46] W. Wu, Q. He, C. Jiang, Nanoscale Res. Lett. 3 (2008) 397.
[47] M. Mahmoudi, S. Sant, B. Wang, S. Laurent, T. Sen, Adv. Drug Deliv. Rev. 63 (2011) 24.
[48] J. Rosen, L. Chan, D. Shieh, F. Gu, Nanomed. Nanotechnol. Biol. Med. 8 (2012) 275.
[49] L. Zhang, W. Dong, H. Sun, Nanoscale 5 (2013) 7664.
[50] T. Hiemstra, Environm. Sci. Nano 5 (2018) 752.
[51] R. Leuchtner, A. Harms, A. Castleman, J. Chem. Phys. 91 (1989) 2753.
[52] M. Knickelbein, S. Yang, S. Riley, J. Chem. Phys. 93 (1990) 94.
[53] I. Billas, A. Châtelain, W. de Heer, Science 265 (1994) 1682.
[54] M. Getzlaff, Fundamentals of Magnetism, Springer Verlag, Berlin, 2008.
[55] D. Mittleman, R. Schoenlein, J. Shiang, V. Colvin, A. Alivisatos, C. Shank, Phys. Rev. B 49 (1994) 14435.
[56] S. Link, M. El-Sayed, J. Phys. Chem. B 103 (1999) 8410.
[57] R. Bailey, A. Smith, S. Nie, Physica E 25 (1985) 1.
[58] P. Buffat, J. Borel, Phys. Rev. A 13 (1976) 2287.
[59] M. Getzlaff, M. Leifels, P. Weber, U. Kökcam-Demir, C. Janiak, SN Appl. Sci. 1 (2019) 489.
[60] GESTIS Substance Database.